On the calibration
of direct-current current transformers

Luca Callegaro, Cristina Cassiago, and Enrico Gasparotto [*†]

Abstract

Modern commercial direct-current current transformers (DCCT) can measure currents up to the kA range with accuracies better than 1×10^{-5}. We discuss here a DCCT calibration method and its implementation with commercial instruments typically employed in low resistance calibration laboratories. The primary current ranges up to $2\,\mathrm{kA}$; in the current range below $100\,\mathrm{A}$ the calibration uncertainty is better than 3×10^{-7}. An example of calibration of a high-performance DCCT specified for primary currents measurement up to $900\,\mathrm{A}$ is discussed in detail.

1. INTRODUCTION

Direct-current current transformers (DCCT) are the most accurate dc high-current sensors commercially available [1], reaching specified relative accuracies in the 10^{-5} range and integral nonlinearities below 10^{-6}. The verification of such high performances and the calibration of the DCCT ratio require metrological facilities capable of handling high currents, with high accuracy and automated operability [2–5].

Ultimate current ratio accuracy is achieved in cryogenic current comparators (CCC) [6]. In a CCC, ratio accuracy is obtained by constraining the magnetic flux (generated by the current being compared) within superconducting shields. An extremely high sensitivity is achieved with a superconducting quantum interference device (SQUID) flux sensor. Even though CCCs capable of handling currents up to $100\,\mathrm{A}$ have been realized [7], these devices are research instruments not available in calibration laboratories.

Ferromagnetic-core, room-temperature current comparators (CC) are current ratio devices which can achieve ratio errors lower than 10^{-7} [8], and can be self-calibrated through step-up procedures [9, 10] with similar levels of uncertainty. Thus, a CC can be employed as current ratio standard in a DCCT calibration setup. Although complex and expensive instruments, high-current CC are common in electrical calibration laboratories, since they are part of commercial resistance ratio bridges employed for the measurement of low-value resistors. These instruments include also current sources, detectors, and firmware for automated operation.

The calibration of the DCCT ratio with a reference current ratio standard (possibly having a different nominal ratio) can be performed by different methods. Recent papers [11, 12] describe a method based on the comparison of the voltages developed by the secondary currents of the devices being compared on calibrated resistance standards.

Here we present a simple method that allows the calibration of the ratio of a DCCT by using commercial components, originally designed for the calibration of low-value resistors. This method does not require calibrated resistance standards; the accuracy, dependent on the primary current, is better than 3×10^{-7} for currents below $100\,\mathrm{A}$. An example of calibration of a DCCT having a $1500 : 1$ nominal ratio for currents up to $900\,\mathrm{A}$ is reported.

The implementation is being employed in the EURAMET.EM-S35 High DC current ratio supplementary comparison [13], in which INRIM acts as co-pilot laboratory.

2. CALIBRATION METHOD

Fig. 1 shows the schematic diagram of the calibration setup which includes three current ratio devices: the DCCT under calibration, an automated current range extender EXT and a current comparator ratio bridge CC.

---

[*]Luca Callegaro, Cristina Cassiago and Enrico Gasparotto are with the Electromagnetism Division of the Istituto Nazionale di Ricerca Metrologica (INRIM), Strada delle Cacce 91, 10135 Torino, Italy, e-mail: l.callegaro@inrim.it
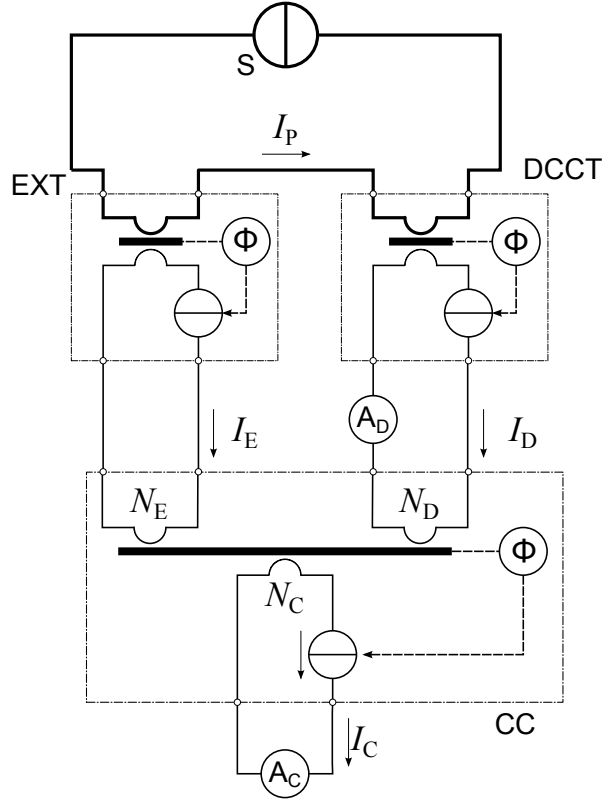
Figure 1: Schematic diagram of the DCCT calibration setup. S is a high-current source, EXT is an automated current range extender and CC is a dc current comparator. The ammeter A_D monitors the DCCT output I_D, while A_C measures the current I_C which is the input quantity of the measurement model (2).

2.1. OPERATION OF CURRENT RATIO DEVICES

The operation of the three current ratio devices, sketched in Fig. 2, is based on the same principle.

$m + 1$ windings are wound around a ferromagnetic core. Each winding k has N_k $(k = 0 \dots m)$ turns, and a current I_k flows through it. The magnetic flux Φ in the core is given by $\mathcal{R}\Phi = \sum_{k=0}^{m} N_k I_k$, where $\mathcal{R}$ is the core magnetic reluctance. Φ is measured by a fluxgate detector [1, 14, 15] whose output constitutes the error signal of a feedback control. The output of the control drives current source I_0, connected to winding 0, to null the flux. The condition $\Phi = 0$ yields the ampere-turns balance equation $\sum_{k=0}^{m} N_k I_k = 0$.

In normal operating conditions, DCCT and EXT have only two ($m = 1$) active windings. The output I_0 of the controlled current source constitutes the device output current; hence, the current I_1 is scaled down with the turns ratio $n_{1,0} = N_1/N_0$ as $I_0 = n_{1,0}I_1$.

In the CC, instead, more windings ($m \geq 2$) are simultaneously active; the currents I_k $(k = 0 \dots m)$ are compared, weighted by their respective turn numbers N_k; the measurement of I_0 gives the CC reading, that is, the residual unbalance between the currents $I_1 \dots I_m$ to be compared.

2.2. CIRCUIT DESCRIPTION

The input windings of both DCCT and EXT are connected in series and driven by the primary current I_P generated by the high-current dc source S. The DCCT and EXT output currents are respectively $I_D = G_D I_P$ and $I_E = G_E I_P$, where G_D is the DCCT current gain (that is, the measurand) and G_E is the
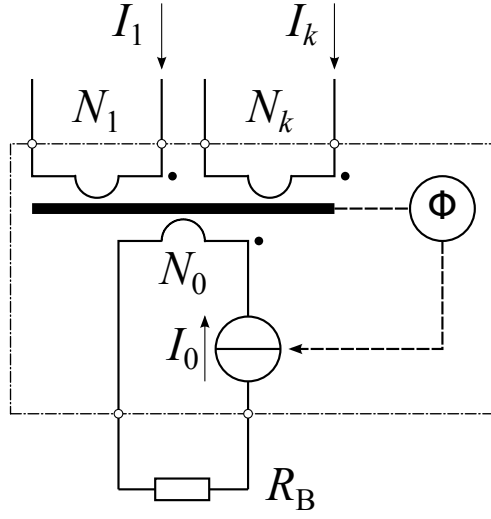
Figure 2: The operating principle of the instruments employed in the calibration setup. $m + 1$ windings, with N_k ($k = 0 \ldots m$) turns each, are wound around a ferromagnetic core (black thick line). The flux detector Φ, through an automatic control (not shown), steers the current source I_0 until $\Phi = 0$; a generic load R_L can be connected to the source.

EXT current gain.

I_D and I_E are connected to two input windings of CC, each having N_D and N_E turns. I_D is also measured by a high-accuracy ammeter A_D.

The CC compensation current I_C, linked to the CC winding with N_C turns, is measured by the ammeter A_C; when operating properly, the CC balance equation is

$$N_E I_E + N_D I_D + N_C I_C = 0. \tag{1}$$

In (1), the sign of turn numbers N_x can be either positive or negative and is set by the winding direction. When in all current ratio devices each core flux is drawn to zero by the corresponding automated control, the balance equation of the whole circuit becomes

$$G_D = \frac{I_C}{I_P} \frac{N_C}{N_D} - G_E \frac{N_E}{N_D}. \tag{2}$$

2.3. MEASUREMENT MODEL
To derive an accurate measurement model, two major nonidealities of the devices employed should be considered:

OFFSET
All instruments based on the fluxgate technique suffer from a certain degree of dc offset, caused by the magnetization hysteresis and relaxation of the ferromagnetic core. This offset, of the order of $10\,\mu\text{A}$ per unit input turn [14], depends on temperature, measurement history and time drifts. To compensate this offset, the reading I_C in (2) is substituted with $\Delta I_C = I_C - I_{C0}$, where I_C is the reading taken at the nominal primary current $I_P^{(n)}$ of interest, and I_{C0} is the reading with null primary current, $I_P = 0$.

RATIO ERRORS
The actual current ratios of CC can differ from the corresponding turn ratios. We call n_{CD} and n_{ED} the current ratios of which N_C/N_D and N_E/N_D are the corresponding nominal turn ratios.
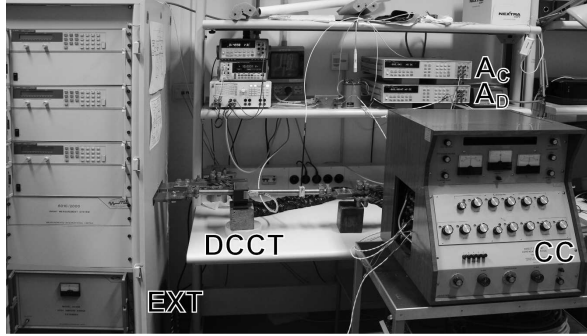
Figure 3: A photo of the implementation of the calibration method. See Sec. 3. and Fig. 1 for the identification of the labels.

Taking into account the above nonidealities, (2) can be rewritten as

$$G_\mathrm{D} = \frac{\Delta I_\mathrm{C}}{I_\mathrm{P}}\, n_\mathrm{CD} - G_\mathrm{E}\, n_\mathrm{ED}, \tag{3}$$

The relative gain error δG_D with respect to the nominal gain $G_\mathrm{D}^{(\mathrm{n})}$ is

$$\delta G_\mathrm{D} = \frac{G_\mathrm{D} - G_\mathrm{D}^{(\mathrm{n})}}{G_\mathrm{D}^{(\mathrm{n})}}. \tag{4}$$

3. IMPLEMENTATION

Fig. 3 shows an implementation of the schematic diagram of Fig. 1. It employs the following instrumentation:

DCCT   The device under test, for which the results reported in Sec. 4. were obtained, is a LEM mod. ITN 900-S ULTRASTAB high-performance current transducer [16]. It handles primary currents $|I_\mathrm{P}| \leq 900\,\mathrm{A}$ with a nominal current ratio $G_\mathrm{D} = 1/1500$. The specified accuracy is better than 2×10^{-5} (including offset), the linearity better than 1×10^{-6}, maximum load resistance $2.5\,\Omega$. Fig. 4 shows the DCCT mounted on the primary busbar.

CC Guildline mod. 9920 direct current comparator [14]. This instrument is particularly versatile since it provides several fixed windings having decadic (1 to 1000) number of turns and one winding with an adjustable number of turns through decade rotary switches; moreover, it allows a full reconfiguration of the connections between the windings and the internal electronics. The settings used in the calibration of the particular DCCT under test are: $N_\mathrm{D} = -100$ (fixed winding), $N_\mathrm{E} = 150$ (decade winding), and $N_\mathrm{C} = 1$ in order to achieve the highest sensitivity in the measurement of I_C.

EXT Two different extenders were employed, depending on I_P:

- Measurement International mod. MI 6011B range extender. Primary current $|I_\mathrm{P}| \leq 100\,\mathrm{A}$, nominal ratio $1/1000$, relative accuracy $< 1 \times 10^{-7}$.

- Measurement International mod. MI 6012M range extender. $|I_\mathrm{P}| \leq 2\,\mathrm{kA}$, nominal ratio $1/1000$, relative accuracy $< 2 \times 10^{-6}$.

    The above specifications were validated in the standard operating setup for low-valued resistor measurements [17].

S Two different sources were employed, depending on the primary current I_P:
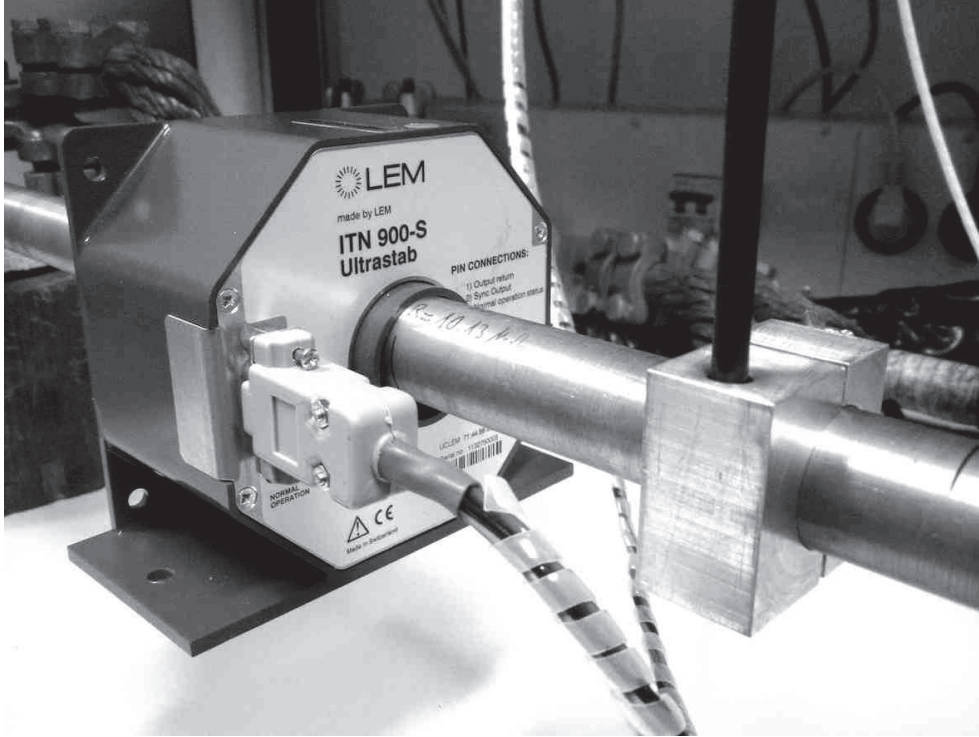
Figure 4: The DCCT under calibration mounted on the primary current busbar. The aluminum block in foreground embeds a Pt100 sensor to monitor the temperature of the primary current busbar.

- Measurement International MI 6100A linear dc power supply, for $|I_P| < 100$ A. Current reversal is achieved with a switch internal to MI 6011B.

- Agilent mod. 6680 (two items in parallel) for $|I_P| < 1750$ A. Current reversal is achieved with a Measurement International mod. 6025 pneumatic switch.

A_D Agilent mod. 3458A multimeter in dc voltage mode, measuring the voltage drop on a Tinsley mod. 1659 $1\,\Omega$ standard resistor.

A_C Agilent mod. 3458A multimeter in dc current mode, 100 mA range.

The DCCT and busbar temperatures are monitored with two Pt100 platinum temperature sensors (see Fig. 4) read by a Fluke mod. 1529 CHUB E-4 thermometer.

4. RESULTS

After a warming-up period of about 1 h at $I_P = +I_P^{(n)}$, I_P is repeatedly cycled between values 0, $+I_P^{(n)}$, 0, $-I_P^{(n)}$ (ending the whole cycle sequence with $I_P = 0$).[1] The reading I_C is continuously recorded. Fig. 5 shows a time series of I_C readings corresponding to an I_P cycle. For each value of I_P, after transients have died out, a time average $\overline{I_C}(I_P)$ is computed (see gray bands in Fig. 5).

The quantity ΔI_C to be employed in Eq. (2) is computed as $\Delta I_C(I_P^{(n)}) = \overline{I_C}(I_P^{(n)}) - (\overline{I_C'}(0) + \overline{I_C''}(0))/2$, where $\overline{I_C'}(0)$ and $\overline{I_C''}(0)$ are the zero readings respectively preceding and succeeding $\overline{I_C}(I_P^{(n)})$ in the time series.

---

[1]It has been found that, for the particular DCCT being tested and for I_P near fullscale, the current must be ramped up smoothly to allow the DCCT automatic shutdown.
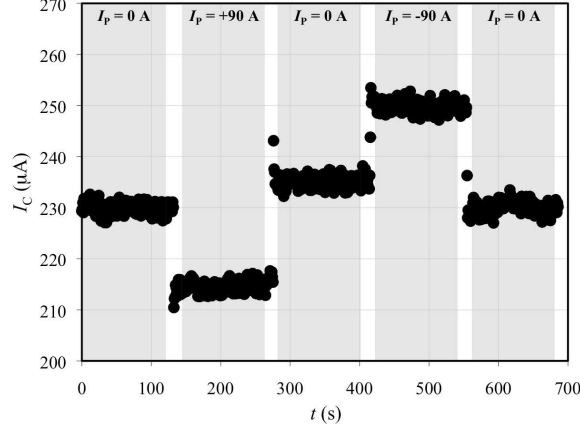
Figure 5: Time recording of the compensation current I_C for different primary currents I_P.

Table 1: DCCT gain G_D for different primary currents I_P. The relative deviation δG_D from nominal ratio is also reported.

$I_P^{(n)}$ A	Supply	EXT	G_D $\times 10^{-4}$	δG_D $\times 10^{-6}$	$U(\delta G_D)$ $\times 10^{-6}$
$+90$	6100A	6011B	6.666 653 9(16)	-1.92	0.24
-90	6100A	6011B	6.666 653 9(16)	-1.92	0.23
$+300$	6680A	6012M	6.666 682(16)	$+2.3$	2.3
-300	6680A	6012M	6.666 676(15)	$+1.5$	2.3
$+600$	6680A	6012M	6.666 677(15)	$+1.6$	2.3
-600	6680A	6012M	6.666 676(15)	$+0.9$	2.3
$+900$	6680A	6012M	6.666 672(15)	$+0.9$	2.3
-900	6680A	6012M	6.666 673(15)	$+1.1$	2.3

From each $\Delta I_C(I_P^{(n)})$, the absolute $\Delta G_C(I_P^{(n)})$ and relative $\delta G_C(I_P^{(n)})$ errors are computed. Fig. 6 graphically shows the values δG_D corresponding to each $I_P^{(n)}$ measurement cycle.

Tab. 1 reports the estimates for G_D and δG_D of the DCCT under measurement, together with the corresponding 95 % expanded uncertainties, for several primary current $I_P^{(n)}$ values.

As an example, the uncertainty budget for the calibration of G_D at $I_P = +90$ A is given in Tab. 2, where it can be appreciated that the main contributions to the measurement uncertainty are due to the instability of I_C and the EXT and CC current ratios G_E and n_{ED}.

5.   CONCLUSIONS

The proposed setup allows the calibration of the ratio of a DCCT with accuracies in the 10^{-6} range or better. The proposed implementation, suitable for primary currents up to 2 kA, is based on commercial instruments typically employed for the calibration of low-valued resistors, and therefore often available in calibration laboratories. The implementation is being employed for the participation to the EURAMET.EM-S35 comparison, which is co-piloted by INRIM and the Federal Institute of Metrology (METAS), Switzerland. The travelling standard of comparison is based on a LEM mod. IT 600-S ULTRASTAB transducer; the participants measure G_D at primary currents $I_P = \pm 90$ A, ± 300 A and ± 600 A. The preliminary characterizations of the travelling standard performed by INRIM and METAS give results which are in agreement within a compound relative uncertainty better than 5×10^{-6}. At the present time the results of the comparison are confidential; a full validation of the INRIM method
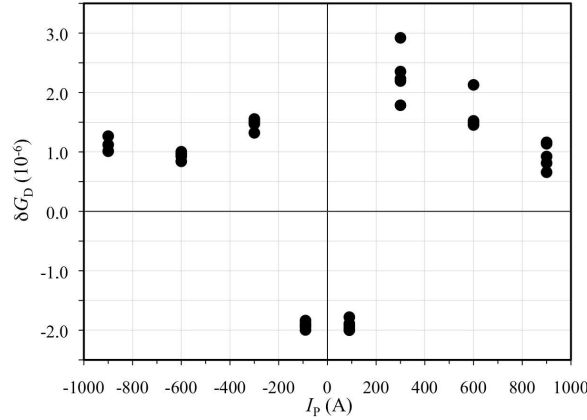
Figure 6: The relative gain error δG_D of the DCCT under calibration, for different nominal primary current values $I_P^{(n)}$. Each dot corresponds to half of the measurement cycle shown in Fig. 5. For each $I_P^{(n)}$, five measurement results are reported. The average value and its uncertainty are given in Tab. 1.

Table 2: Uncertainty budget for G_D, at $I_P^{(n)} = +90$ A.

Quantity	X	$u(X)$	contrib. to $u(G_D)$	type	note
ΔI_C	$-17.2\,\mu A$	$0.36\,\mu A$	2.7×10^{-11}	A	Standard deviation of the mean, taken over 5 I_P cycles
I_P	$90\,A$	$90\,mA$	1.3×10^{-12}	B	A_D readings (bound on maximum error)
n_{CD}	$-6.666\,666\,7 \times 10^{-3}$	6.7×10^{-10}	$< 1 \times 10^{-13}$	B	CC manufacturer's specifications
n_{ED}	$-6.666\,666\,7 \times 10^{-1}$	6.7×10^{-8}	6.7×10^{-11}	B	CC manufacturer's specifications
G_E	$+1.000\,000\,0 \times 10^{-3}$	5.8×10^{-11}	3.8×10^{-11}	B	EXT (MI 6011B) manufacturer's specifications
G_D	$+6.666\,653\,9 \times 10^{-4}$	8.1×10^{-11}			
δG_D	-1.92×10^{-6}	1.2×10^{-7}			
$U(\delta G_D)$		2.4×10^{-7}			Expanded uncertainty, 95 % coverage probability

will become available after the publication of the comparison report, expected by the end of 2015.

REFERENCES

[1] P. Ripka, "Electric current sensors: a review," *Meas. Sci. Technol.*, vol. 21, p. 112001, 2010, 23 pp.

[2] M. Zhu and K. Xu, "A calibrating device for large direct current instruments up to 320 kiloampere-turns," *Instrumentation and Measurement, IEEE Transactions on*, vol. 47, no. 3, pp. 711–714, Jun 1998.

[3] G. Fernqvist, J. Pett, and J. Pickering, "A reference standard system based on dc current," in *Precision Electromagnetic Measurements, 2002. Conference Digest 2002 Conference on*, June 2002, pp. 164–165.

[4] G. Fernqvist, B. Halvarsson, J. Pett, and J. Pickering, "A novel current calibration system up to 20

kA," *Instrumentation and Measurement, IEEE Transactions on*, vol. 52, no. 2, pp. 445–448, April 2003.

[5] G. Hudson, B. Jeckelmann, and J.-D. Baumgartner, "Comparison of cern and metas high current standards up to 10ka," in *Precision Electromagnetic Measurements Digest, 2008. CPEM 2008. Conference on*, June 2008, pp. 548–549.

[6] J. M. Williams, "Cryogenic current comparators and their application to electrical metrology," *IET Science, Measurement & Technology*, vol. 5, no. 6, pp. 211–224, 2011.

[7] J. M. Williams and P. Kleinschmidt, "A cryogenic current comparator bridge for resistance measurements at currents of up to 100 A," *IEEE Trans. Instr. Meas.*, vol. 48, no. 2, pp. 375–378, 1999.

[8] W. J. M. Moore and P. N. Miljanic, *The current comparator*, ser. IEE electrical measurement series. London, UK: Peter Peregrinus Ltd, 1988, vol. 4, iSBN 0863411126.

[9] H. Shao, F. Lin, X. Hua, B. Liang, K. Qu, and Y. Pan, "DC high current ratio standard based on series-parallel calibration method," in *Precision Electromagnetic Measurements (CPEM) Conf.*, Jun. 2010, pp. 535 –536.

[10] H.-G. Zhao, X.-Z. Zhang, Y. Liu, L.-Y. Zheng, and B.-X. Zou, "Calibration of DC current up to 600 A," in *Precision Electromagnetic Measurements (CPEM) Conf. on*, Jun. 2010, pp. 603 –604.

[11] B. Jeckelmann, "Genauigkeit von Gleichstrom-messungen bis 20 kA im ppm-Bereich," *metINFO Zeitsch. für Metrol.*, vol. 11, no. 3, pp. 4–8, 2004.

[12] G. Rietveld, J. H. N. van der Beek, M. Kraft, R. E. Elmquist, A. Mortara, and B. Jeckelmann, "Low-ohmic resistance comparison: Measurement capabilities and resistor traveling behavior," *IEEE Trans. Instr. Meas.*, vol. 6, no. 6, pp. 1723–1728, 2013.

[13] C. Cassiago and A. Mortara, "Comparison of high-current ratio standard," EURAMET, Technical Protocol 1217, Feb 2012, available online at www.euramet.org.

[14] M. P. MacMartin and N. L. Kusters, "A direct-current-comparator ratio bridge for four-terminal resistance measurements," *IEEE Trans. Instr. Meas.*, vol. 15, no. 4, pp. 212 –220, Dec 1966.

[15] P. Odier, "DCCT technology review," in *Proc. of Workshop on DC current transformers and beam-lifetime evaluations*, A. Peters, H. Schmickler, and K. Wittenburg, Eds. Lyon, France: CARE-HHH-ABI Networking, 1-2 Dec 2004, pp. 3–5.

[16] W. Teppan and D. Azzoni, "Closed-loop fluxgate current sensor," European Patent EP2 251 704A1, 2010.

[17] M. Kraft, "Measurement techniques for evaluating current range extenders from 1 ampere to 3000 ampere," *NCSLI Measure J. Meas. Sci.*, vol. 7, no. 3, pp. 32–36, Sep 2012.